PHYSICAL REVIEW A VOLUME 9, NUMBER 1 JANUARY 1974

# Channel interaction and threshold behavior of photoionization*

C. D. Lin
*Department of Physics, The University of Chicago, Chicago, Illinois 60637*
(Received 15 February 1973)

Channel interaction is shown to have a substantial effect of "spectral repulsion" that distorts the photoionization spectrum near the threshold of a weak channel. This effect is illustrated by calculating numerically the cross section of the $3s \rightarrow \epsilon p$ transition of Ar, taking into account its coupling with the $3p \rightarrow \epsilon d$ transition. The result is very different from that obtained by an independent-particle approximation. Examples calculated by other authors on He, Ne, and Xe serve as additional illustrations.

## I. INTRODUCTION

The cross sections for scattering or reaction processes generally show rapid variations, as functions of energy, at the threshold where a new channel opens. In a wide class of processes, like the photoproduction of particles, with no Coulomb interaction between the final products, the cross section has infinite derivative at the threshold. This singular behavior, known as a "Wigner cusp,"[1] is the result of the sudden opening of a new channel. In a number of other processes, like the photoionization of atoms, there is Coulomb interaction between the final products. It is known that no singularity occurs in the cross sections. In an attractive Coulomb field, there exist virtual bound states (forming Rydberg series) when the incident energy is still below the threshold. The density of bound states increases rapidly [in proportion to $(n-\mu)^3$, where $n$ is the principal quantum number and $\mu$ is the quantum defect] as the energy of the incident particle approaches the reaction threshold. Because of the presence of these virtual bound states, the opening of a new channel in a Coulomb field is a gradual process, and therefore the threshold behavior is altered. Nevertheless, the opening of a new channel can perturb substantially the relative cross sections for different reaction channels. It is the objective of this paper to study the cross section for photoionization of atoms into different channels, corresponding to different levels of the ion, near the threshold of a new channel.

Partial information about the cross section near the threshold of a new channel can be obtained from the properties of virtual bound states. These bound states are stationary only within an independent-particle approximation. Interactions between the particles actually cause these bound states to autoionize into the continuum. Autoionization is an example of the transitions between channels that are classified as effects of "interchannel interaction." Channel interaction exists over the whole spectrum, but its effects are particularly apparent where the bound states of one channel overlap the continuum of another channel; the line profiles resulting in this case have been studied by Fano[2] and by Fano and Cooper[3] within this context. The theory considers separate amplitudes for transition to the continuum directly from the ground state and through the quasistationary bound state. The transition probability, as detailed by Fano and Cooper,[4] can be broken into four terms, which represent contributions: from the direct transition to the continuum, from the transition through the discrete state, from an interference term between these two amplitudes, and from a term called spectral repulsion. The interference term accounts for the asymmetry of the line profile; the spectral repulsion term has the effect of depressing the direct transition probability in the vicinity of the line.

Single autoionizing states were treated earlier,[2] but the levels of neutral atoms or ions generally belong to Rydberg series and each series should be treated as a whole, together with the continuum adjoining the series limit. The autoionization of a whole Rydberg series has been discussed briefly by Fano and Cooper.[3] Experimentally, in the higher levels of a Rydberg series we are interested in the total cross section averaged over a spectral range that includes many lines. As shown in Ref. 3 (especially p. 1371), the average total cross section also has terms representing the effects of interference and spectral repulsion. This is not surprising if one recognizes that interference and spectral repulsion, as results of interchannel interaction, must be present over the whole energy range where the two channels interact.

Interchannel interaction always produces a readjustment of the results of an independent-particle calculation. Its strength is indicated by the magnitude of the residual interaction, which couples the two channels and is often weak. Never-

theless, interchannel interaction may have large effects in narrow spectral regions. In particular, interference between the independent-particle amplitudes contributing to the cross section of different channels becomes conspicuous throughout the spectral range, where one channel has singular features, such as discrete lines, a threshold, or a combination of them, because its effect varies rapidly along the spectrum. In spectral ranges without singular features the effects of interference are not obvious in the spectrum, but can be detected only by comparing quantitative experimental cross sections with theoretical cross sections calculated in the independent-particle approximation. Actually the combination "threshold plus Rydberg series" may be viewed as a single large singular spectral feature. Interference should become inconspicuous only far below the first autoionizing Rydberg line or far above the threshold.

The effect of spectral repulsion between two channels is quite familiar in discrete spectra, when a level of one configuration (or channel) lies in the midst of another configuration; configuration interaction (or interchannel interaction) causes the energy levels of the second configuration to be shifted away from the perturbing level. In the autoionization of a Rydberg series, spectral repulsion manifests itself in the sense that the oscillator strength of the continuum is thinned out in the proximity of the discrete levels. In the energy region where two or more channels are open, spectral repulsion readjusts the distribution of oscillator strength between the channels. This readjustment should be very obvious throughout the range where the opening of a new channel constitutes a singularity in the spectrum.

The effect of interchannel interaction on the calculations of photoionization cross sections was discussed qualitatively by Fano and Cooper,[4] but has been studied only recently. While the present work was in progress, a series of calculations on the same subject was reported by Amusia *et al.*[5] This paper is presented nevertheless because it starts from a different point of view and particularly because its calculation is designed to display separately various contributions to the effect of channel coupling. The results of the various calculations appear consistent and in agreement with experiment, as will be detailed below.

In this paper, we see how the cross section of the $3s \rightarrow \epsilon p$ ($\epsilon$ is the photoelectron energy) photoionizing transition in Ar is changed by the channel coupling with the $3p \rightarrow \epsilon d$ transition. We are particularly interested in the energy region near the threshold of the $3s \rightarrow \epsilon p$ process ($\hbar\omega \sim 30$ eV), where independent-particle-model calculations show the cross section of the direct single-channel $3s \rightarrow \epsilon p$ transition to be small, and where the main contribution to the total cross section comes from $3p \rightarrow \epsilon d$ transition. Calculations of the $3s \rightarrow \epsilon p$ transition have been performed by Cooper and Manson[6] using wave functions generated from the Herman-Skillman model potential,[7] and by Kennedy and Manson[8] using Hartree-Fock wave functions. Although their results disagree in magnitude, both calculations show the cross section to be small and to increase monotonically with energy near the threshold. We will show that addition of interchannel coupling to the direct transition changes the threshold behavior of $3s \rightarrow \epsilon p$ completely. The inclusion of interchannel interaction is equivalent to removal of a $3s$ electron through an intermediate virtual excitation of the $3p$ subshell, i.e., through a transition $3s^2 3p^6 \rightarrow 3s^2 3p^5 \epsilon' d \rightarrow 3s 3p^6 \epsilon p$, where $\epsilon'$ is the energy of the virtually excited electron.

In Sec. II, the final-state interaction between photoelectron and ion core is taken into consideration by a reaction-matrix method. This method has been applied by Starace[9] to a single-channel problem in calculating the photoionization cross section of Ar from the $3p$ subshell and of Xe from $4d$ subshell. The general formulation is given here for an arbitrary $N$-channel problem, but explicit results are given for our two-channel problem in order to bring out the significant features of channel interaction. Section III gives the results of a numerical calculation for the photoionization cross section of the $3s \rightarrow \epsilon p$ transition of Ar. The interaction of the final state channel $3s 3p^6 \epsilon p\, {}^1P^0$ with $3s^2 3p^5 \epsilon' d\, {}^1P^0$ is included by the method of Sec. II. The calculation in Sec. III improves the final-state wave function only; the ground-state wave function is not improved. The cross section thus calculated is compared with the result of an independent-particle approximation, where neither the ground-state nor final-state wave function are improved. The significant difference of the cross sections for these two calculations near the $3s$ threshold indicates the importance of interchannel coupling. The departure from the results of the independent-particle calculation is interpreted as due to spectral repulsion resulting from channel interaction. Section IV gives a brief discussion of how to include an improvement of the ground-state wave function in a simple and effective way. This is done by using a simplified method of random-phase approximation with exchange. The resulting equations are very similar to the formulas of Sec. II. The result of this calculation is then compared with those in Ref. 5. In Sec. V we show other examples that can be understood in terms of interchannel interaction.

## II. THEORY

The calculation of photoionization cross sections requires accurate wave functions of the initial state and of the final state of the electron-plus-ion system. The cross section is given by

$$\sigma_i = \tfrac{4}{3}\pi a_0^2 \alpha \omega \left| \langle \psi_{iE} | \sum_j z_j | \psi_G \rangle \right|^2 , \tag{1}$$

for transition to a particular channel $i$. Atomic units are used throughout this paper and in this formula $a_0$ is the Bohr radius, $\alpha$ is the fine-structure constant, $\omega$ is the photon energy in atomic units, $\psi_{iE}$ is the final-state wave function for channel $i$ with total energy $E$, normalized per unit energy, and $\psi_G$ is the wave function of the initial state from which photoionization occurs. The summation of $j$ extends over all the electrons in the atom.

The wave function of the atom is to be constructed as a linear combination of antisymmetrized products of single-particle wave functions. The choice of these basis functions is detailed elsewhere.[10] Briefly, we split the spin-independent total Hamiltonian $H$ of the atom,

$$H = \sum_i \left( -\frac{1}{2}\nabla_i^2 - \frac{Z}{r_i} \right) + \sum_{i>j} \frac{1}{r_{ij}} ,$$

into a model Hamiltonian

$$H_{\text{mod}} = \sum_i \left[ -\tfrac{1}{2}\nabla_i^2 + V_{\text{HS}}(r_i) \right]$$

and a residual interaction $V_{\text{res}}$

$$V_{\text{res}} = -\sum_i \left( \frac{Z}{r_i} + V_{\text{HS}}(r_i) \right) + \sum_{i>j} \frac{1}{r_{ij}} ,$$

where $V_{\text{HS}}$ is a local potential tabulated by Herman and Skillman.[6] The basis set for the many-electron wave functions of the atom consists of an infinity of antisymmetrized solutions $u_{iE}$ of $H_{\text{mod}}$. The subscript $E$ in $u_{iE}$ indicates the total energy of the atom (or electron-plus-ion system); $i$ is a set of discrete quantum numbers that are required besides $E$ to identify $u_{iE}$. Each $i$ of the discrete set identifies a different channel. Note that the channels cannot be classified without reference to the independent-particle model. An eigenstate of the total Hamiltonian $H$ is represented as a linear combination of these basis functions, i.e.,

$$\psi_E = \sum_i \int dE' \, a_{iE'}(E) u_{iE'} , \tag{2}$$

where the integral over the energy $E'$ is understood to include a summation over discrete energy states.

In the following, we concentrate on the final-state wave function of the electron-plus-ion system. Following the method of Sec. 6.2 of Ref. 4, we represent the coefficients $a_{iE'}(E)$ in terms of the elements of a reaction matrix $K$, which represents the effect of final-state interaction between the photoelectron and the ion,

$$a_{iE'}(E) = P(E-E')^{-1} \sum_j K_{iE',jE}(E) B_j(E) + \delta(E'-E) B_i(E) . \tag{3}$$

In this formula, $P$ indicates that principal-part integration is to be taken at $E'=E$ when $a_{iE'}(E)$ is substituted into Eq. (2). The coefficients $B_i(E)$ will be determined by the boundary condition appropriate to the photoionization process.

The wave function $\psi_E$ is then given in terms of $K$-matrix elements and coefficients $B_i$ as

$$\psi_E = \sum_i \left( u_{iE} B_i(E) + \sum_j P \int \left[ u_{iE'} K_{iE',jE}(E)/(E-E') \right] dE' B_j(E) \right) , \tag{4}$$

where the matrix element $K_{iE',jE}(E)$ satisfies the coupled integral equations

$$K_{iE',jE}(E) = V_{iE',jE} + \sum_l \int dE'' \, V_{iE',lE''} [P/(E-E'')] K_{lE'',jE}(E) , \tag{5}$$

with

$$V_{iE',jE} = \langle u_{iE'} | V_{\text{res}} | u_{jE} \rangle .$$

To determine $B_i(E)$, we examine the asymptotic behavior of the wave function $\psi_E$ of the system when the electron is very far away from the ion core. The asymptotic behavior of the basis function $u_{iE'}$ is represented as

$$u_{iE'} \xrightarrow[r\to\infty]{} C_i r^{-1} \sin[k_i r + \Theta_i] , \tag{6}$$

with

$$\Theta_i = k_i^{-1} \ln(2k_i r) - \tfrac{1}{2} l_i \pi + \arg\Gamma(l_i + 1 - i/k) + \delta_i .$$

In this equation $k_i = k_i(E')$, $\delta_i$ is the phase shift due to the short-range (non-Coulomb) part of the HS potential, $r$ is the distance of the photoelectron from the ion core. The photoelectron has orbital angular momentum $l_i$ and kinetic energy $\frac{1}{2}k_i^2$. The wave function of the core electrons, the spin of the photoelectron, and the normalization factor are represented together by $C_i$. Antisymmetriza-

tion of the photoelectron and core-electron variables is implied but not explicitly indicated in (6).

The asymptotic form of $\psi_E$ is obtained by substituting (6) into (4) to give

$$\psi_E \xrightarrow[r\to\infty]{} \sum_i \frac{C_i}{r}\left(\sin(k_i r+\Theta_i)B_i(E)+[-\pi\cos(k_i r+\Theta_i)]\sum_j K_{iE,jE}(E)B_j(E)\right).$$

This expression is now represented in terms of ingoing and outgoing waves of the photoelectron by

$$\psi_E \xrightarrow[r\to\infty]{} \sum_i \frac{C_i}{r}\left[-\frac{1}{2}\left(iB_i(E)+\pi\sum_j K_{ij}(E)B_j(E)\right)e^{i(k_i r+\Theta_i)}+\frac{1}{2}\left(iB_i(E)-\pi\sum_j K_{ij}(E)B_j(E)\right)e^{-i(k_i r+\Theta_i)}\right],$$

where $K_{ij}(E)\equiv K_{iE,jE}(E)$ indicates the $K$-matrix elements diagonal in energy, i.e., "on the energy shell."

The boundary condition appropriate to observation of the photoelectron in channel $\bar{i}$ requires that the outgoing-wave part of all channels $i\neq\bar{i}$ vanish. That is, the coefficient in front of $e^{i(k_i r+\Theta_i)}$ for $i\neq\bar{i}$ must be equal to zero, and that in front of $e^{i(k_{\bar{i}} r+\Theta_{\bar{i}})}$ must be equal to unity. For an $N$-channel problem this condition gives $N$ linear algebraic equations whose solution gives the $N$ unknowns $B_i(E)$.

For our purpose, we want to examine the case of a two-channel problem. When channel 1 is to be observed, we obtain

$$B_1^{(1)}(E)=\frac{[1-i\pi K_{22}(E)]}{\Delta(E)},$$

$$B_2^{(1)}(E)=\frac{i\pi K_{21}(E)}{\Delta(E)},$$

where

$$\Delta(E)=\det|1-i\pi K(E)|$$
$$=[1-i\pi K_{11}(E)][1-i\pi K_{22}(E)]$$
$$+\pi^2 K_{12}(E)K_{21}(E). \tag{7}$$

The eigensolution for a two-channel problem with observation in channel 1 is then

$$\psi_E^{(1)}=\frac{1-i\pi K_{22}}{\Delta(E)}\left(u_{1E}+P\int dE'\frac{u_{1E'}K_{1E',1E}}{E-E'}+P\int dE'\frac{u_{2E'}K_{2E',1E}}{E-E'}\right)$$
$$+\frac{i\pi K_{21}}{\Delta(E)}\left(u_{2E}+P\int dE'\frac{u_{2E'}K_{2E',2E}}{E-E'}+P\int dE'\frac{u_{1E'}K_{1E',2E}}{E-E'}\right). \tag{8}$$

The dipole amplitude for transition to channel 1 is given by

$$D^{(1)}(E)=\frac{1-i\pi K_{22}}{\Delta(E)}\left(d_{1E}+P\int dE'\frac{d_{1E'}K_{1E',1E}}{E-E'}+P\int dE'\frac{d_{2E'}K_{2E',1E}}{E-E'}\right)$$
$$+\frac{i\pi K_{21}}{\Delta(E)}\left(d_{2E}+P\int dE'\frac{d_{1E'}K_{1E',2E}}{E-E'}+P\int dE'\frac{d_{2E'}K_{2E',2E}}{E-E'}\right), \tag{9}$$

where $d_{iE}=\langle\psi_G|\sum_j z_j|u_{iE}\rangle$. A similar equation for the dipole transition amplitude to channel 2 can be obtained by interchanging the indices 1 and 2 in Eq. (9).

From Eq. (9), we see that the problem of calculating dipole amplitudes requires the solution of the system of integral equations (5) for $K$-matrix elements. It is to be noted that no approximation at all has been imposed in this formulation, except for restricting the number of channels. We do *not* require the residual interaction to be small.

Equation (9) displays the effect of interchannel coupling clearly. In particular, the spectral distribution of a channel (say channel 1) with a small dipole transition amplitude $d_{1E}$ in the independent-particle approximation will be changed significantly by the effect of interchannel coupling with a channel (say channel 2) with large $d_{2E'}$. In Eq. (9), the effect of interchannel interaction upon the transformed dipole matrix element $D^{(1)}(E)$ can be separated into two parts; one is given by the second line of Eq. (9), which is an "on-the-energy-shell" effect, and the other is given by the last principal-part integral $P\int dE'\, d_{2E'}K_{2E',1E}/(E-E')$ of the first line, which is an "off-the-energy-shell" effect. Information about the importance of the interaction "on the shell" can be obtained through experimental observation on the line profile of autoionizing states, since the linewidth provides an estimate of the magnitude of $K_{21}$.[11] However, a

small $K_{21}$ does not guarantee that the effect of interchannel interaction is small. The "off-the-energy-shell" part can be important if the principal-part integral $P\int dE' d_{2E'} K_{2E',1E}/(E-E')$ is not small compared with $d_{1E}$. The contribution of the dipole transition amplitude $d_{2E'}$ to the $D^{(1)}(E)$ of channel 1 given by this integral is to be called an effect of spectral repulsion. It results from admixture into $\psi_E^{(1)}$ of channel 2 wave functions $u_{2E'}$, whose energy $E'$ is *different* from the energy $E$ of channel 1. Notice that the influence of spectral repulsion upon the photoionization cross section can be singled out only by explicit calculation of $d_{1E}$, $d_{2E'}$, and $K_{2E',1E}$, as contrasted with any direct calculation of $D_E^{(1)}$ that fails to separate the various terms of (9). Rapid variation of the product $d_{2E'}K_{2E',1E}$ as a function of $E'$ increases the value of $P\int dE' d_{2E'}K_{2E',1E}/(E-E')$, and thus implies importance of spectral repulsion by channel 2 upon the photoionization cross section of channel 1.

## III. NUMERICAL RESULTS FOR THE Ar $3s \to \epsilon p$ PHOTOIONIZATION

In this section we calculate the photoionization cross section of Ar from the $3s$ and $3p$ subshells, taking into consideration the interchannel interaction of the final-state wave functions. As the photon energy $\hbar\omega$ exceeds the $3s$ subshell ionization threshold ($I_{3s}=29.5$ eV), either a $3s$ or a $3p$ electron can be ionized. The photoelectron may leave the $Ar^+$ ion with kinetic energy $\epsilon_1=\hbar\omega-I_{3s}$ or $\epsilon_2=\hbar\omega-I_{3p}$ ($I_{3p}=15.6$ eV). The *ab initio* calculation in this section contains the following assumptions.

(i) Photoionization from $3p$ to $\epsilon s$ is neglected, only the transition from $3p$ to $\epsilon d$ being considered. This simplification is justified by the results of independent-particle calculation, showing the $3p \to \epsilon s$ cross section to be an order of magnitude smaller than the $3p \to \epsilon d$ cross section. Furthermore, the dipole transition amplitude of the $3p \to \epsilon s$ process is smooth, which should further reduce the effect of the coupling of the $3p \to \epsilon s$ transition with $3s \to \epsilon p$ transition, as is apparent from the discussion of Eq. (9).

(ii) The core electrons remain unexcited during the photoionization process. Hence the single-particle wave functions of the core electrons in the final state are the same as that of the ground state, being eigenfunctions of the model Hamiltonian $-\frac{1}{2}\nabla_i^2+V_{\rm HS}(r_i)$, with appropriate sets of discrete quantum numbers.

(iii) The wave function of the initial $3s$ or $3p$ electron is calculated directly from the model Hamiltonian. No attempt is made in this section to improve the wave function of the initial state. This approximation will be partly removed in Sec. IV.

With the foregoing assumptions, the photoionization of Ar with photon energy above the $3s$ ionization threshold is approximated by a two-channel problem, consisting of $3s \to \epsilon p$ and $3p \to \epsilon d$ transitions. The basis set for the final-state wave functions comprises an infinity of Slater determinants

$$u_{1E} = |1s^2 2s^2 \cdots 3s 3p^6 \epsilon_1 p\, {}^1P^0\rangle$$

and

$$u_{2E} = |1s^2 2s^2 \cdots 3s^2 3p^5 \epsilon_2 d\, {}^1P^0\rangle .$$

The channel index $i (i=1,2)$ also indicates the orbital angular momentum of the photoelectron. Capital letters $E$, $E'$, $E''$ are used for the total energy of the photoelectron-plus-ion system; $\epsilon$, $\epsilon'$, and $\epsilon''$ are used for the kinetic energy of the photoelectron when it is far away from the ion. An unprimed energy index refers to the state reached by photoionization, while primed energy indices refer to virtual intermediate states in the calculation. The zero level of the total energy is so chosen such that the magnitude of $E$ is equal to the kinetic energy $\epsilon_2$ of the $3p \to \epsilon_2 d$ transition; The kinetic energy $\epsilon_1$ of the photoelectron in channel 1 is given by $\epsilon_1 = E-(I_{3s}-I_{3p})$ for a given total energy $E$. The photon energy $\omega$, which gives a system with total energy $E$, is $\omega = I_{3p}+E$.

The calculation of dipole matrix elements in Eq. (9) requires us to solve Eq. (5) for the $K$-matrix elements. This can be done separately for final states of channel 1 and of channel 2. For channel 1, we solve the coupled equations

$$K_{i\epsilon',1\epsilon} = V_{i\epsilon',1\epsilon} + P\int \frac{V_{i\epsilon',1\epsilon''}K_{1\epsilon'',1\epsilon}}{\epsilon-\epsilon''}d\epsilon'' + P\int \frac{V_{i\epsilon',2\epsilon''}K_{2\epsilon'',1\epsilon}}{\epsilon-\epsilon''-I_{3s}+I_{3p}}d\epsilon'' , \tag{10}$$

with $i=1,2$ and for channel 2 we solve

$$K_{i\epsilon',2\epsilon} = V_{i\epsilon',2\epsilon} + P\int \frac{V_{i\epsilon'1\epsilon''}K_{1\epsilon'',2\epsilon}}{\epsilon-\epsilon''-I_{3p}+I_{3s}}d\epsilon'' + P\int \frac{V_{i\epsilon',2\epsilon''}K_{2\epsilon'',2\epsilon}}{\epsilon-\epsilon''}d\epsilon'' . \tag{11}$$

with $i=1,2$. In Eqs. (10) and (11), we use $K_{i\epsilon',j\epsilon}$ to represent $K_{i\epsilon',j\epsilon}(E)$ for a given total energy $E$. The intermediate states $\epsilon'$ and $\epsilon''$ include bound states as well as the continuum states. The integral in (10) and (11) is understood to include a sum over these discrete states.

For a given energy $E$, the calculation is done separately for channel 1 with $\epsilon = E - I_{3s} + I_{3p}$ and channel 2 with $\epsilon = E$. For a given $\epsilon$ of channel 1, the coupled integral equation is solved by reducing the linear integral equations to algebraic equations, which can then be solved by standard matrix-inversion methods. The principal-part integral in Eq. (10) is expressed as a finite sum, with the high-energy cutoff chosen at 3.505 a.u. for channel 1, and 4.0 a.u. for channel 2. The resulting energy range is then divided into a mesh. A proper way of treating the principal-part integral in this continuum energy range and of summing the infinite discrete energy states has been explained by Altick and Moore.[12] Using this method, we choose 12 mesh points for channel 1, and 18 mesh points for channel 2. The solution of the resulting algebraic equations obtained from Eq. (10) involves the inversion of a matrix with dimension $30 \times 30$. Equation (11) is solved in the same way.

After choosing the mesh points we have to evaluate the matrix elements of the residual interaction. For the intrachannel interaction matrix elements $V_{i\epsilon',i\epsilon}(i = 1, 2)$, the numerical procedure is discussed by Starace.[9] For the interchannel interaction matrix elements

$$V_{2\epsilon',1\epsilon} \equiv \langle 1s^2 \cdots 3s^2 3p^5 \epsilon' d\ {}^1P^0 | V_{\rm res} \times | 1s^2 \cdots 3s 3p^6 \epsilon d\ {}^1P^0 \rangle ,$$

the angular integral can be evaluated exactly[13] and we find

$$V_{2\epsilon',1\epsilon} = \tfrac{1}{3}\sqrt{2}\,[-R^{(1)}(3s\epsilon' d, 3p\epsilon p) + 2R^{(1)}(3s\epsilon' d, \epsilon p 3p)],$$

with $R^{(1)}(ab, cd)$ defined as

$$R^{(1)}(ab, cd) = \int_0^\infty dr_1 \int_0^\infty dr_2 \frac{r_<^l}{r_>^{l+1}} \times R_a(r_1) R_b(r_2) R_c(r_1) R_d(r_2), \qquad (12)$$

where $r_>$ and $r_<$ are the greater and lesser of $r_1$ and $r_2$. $R_a$ is a real radial wave function of the electron in state $a$, generated numerically using the Herman-Skillman potential $V_{\rm HS}$ for Ar. $R^{(1)}(ab, cd)$ is obtained by integrating Eq. (12) numerically.

The dipole transition amplitudes $D^{(1)}(E)$ and $D^{(2)}(E)$ are obtained by performing the principal-part integration in Eq. (9). Within the approximations of this section, we have

$$d_{1\epsilon} = \sqrt{2} \int_0^\infty R_{\epsilon p}(r) r R_{3s}(r)\, dr$$

and

$$d_{2\epsilon} = 2 \int_0^\infty R_{\epsilon d}(r) r R_{3p}(r)\, dr .$$

The cross section calculated for the $3p \rightarrow \epsilon d$ transition is found to be almost unchanged by the interchannel coupling with the $3s \rightarrow \epsilon p$ transition. In fact, the result departs no more than 10% from the result[9] of a single-channel calculation. This is not surprising because the dipole amplitude for $3p \rightarrow \epsilon d$ transitions is an order of magnitude greater than that of $3s \rightarrow \epsilon p$ transitions in the energy range considered here. The small amplitude of $3s \rightarrow \epsilon p$ transitions cannot contribute a significant amount to the $3p \rightarrow \epsilon d$ cross section, even when the coupling is not small.

On the other hand, the effect of interchannel coupling with the $3p \rightarrow \epsilon d$ transitions will have significant effect on the cross section of $3s \rightarrow \epsilon p$ transition if the coupling is not too small. In Fig. 1, we present the Ar $3s \rightarrow \epsilon p$ transition cross section calculated from $D^{(1)}(E)$ and from $d_{1E}$, that is, with and without taking into account the interchannel interactions with $3p \rightarrow \epsilon d$ channel. We see that the spectral distribution just above the $3s$ threshold differs qualitatively for the two calculations. The cross section, instead of rising smoothly from the threshold, as predicted by the independent-particle approximation, is found to have a rather rapid variation with energy near the threshold in the coupled-channel calculation. The existence of a dip and rapid variation with energy of the calculated cross section should be regarded as the main result of this calculation.

In order to understand the difference between the

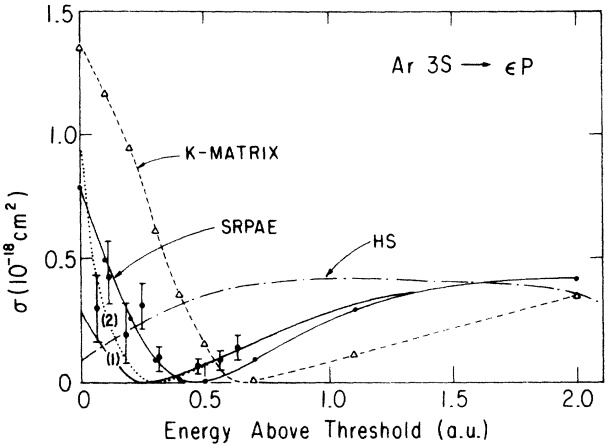


FIG. 1. △, ●, results of numerical calculation; ---, interpolated results of $K$-matrix method (Sec. III); ——, interpolated results of SRPAE method (Sec. IV); -·-·, results of Ref. 6 (Herman-Skillman model). Curve (1): result of Amusia *et al.* (Ref. 5); curve (2): result of Amusia *et al.* (Ref. 17). The experimental data are taken from Lynch *et al.* (Ref. 16).

two calculations, we study the various terms in Eq. (9). In particular, the last principal-part integral of the first line of Eq. (9) gives a large contribution, as shown in Table I. This term is classified in Sec. II as representing the "off-the-energy-shell" part of the effect of interchannel interaction and can be written in the form

$$P\int d\epsilon'\, d_{2\epsilon'}K_{2\epsilon',1\epsilon}/(\epsilon-\epsilon'-I_{3s}+I_{3p})$$

in terms of the energy $\epsilon'$ of the photoelectron in the $\epsilon' d$ channel.

The large value of this principal-part integral results from the rapid variation of the numerator of the integrand $d_{2\epsilon'}K_{2\epsilon',1\epsilon}$ across the singularity. Table II shows some of the matrix elements $K_{2\epsilon',1\epsilon}$ calculated from Eq. (10). We see that the matrix elements decrease monotonically with energy $\epsilon'$ of the $3p \to \epsilon' d$ transition for a given $\epsilon$. Since $d_{2\epsilon'}$ also decreases monotonically (in absolute value) over a wide range of energy, the product $d_{2\epsilon'}K_{2\epsilon',1\epsilon}$ decreases (in absolute value) rather fast with the energy $\epsilon'$; this makes the integral quite large compared with $d_{1\epsilon}$. In fact, the calculation shows that $D^{(1)}(E)$ is dominated near the threshold by the value of this principal-part integral. This integral is negative and has absolute value much larger than $d_{1\epsilon}$. This explains why the cross section near threshold calculated from $D^{(1)}(E)$ is larger than that calculated from $d_{1\epsilon}$. However, the absolute value of this integral decreases rapidly with energy $\epsilon$ because $K_{2\epsilon',1\epsilon}$ decreases rapidly with $\epsilon$, as can be seen from Table II. Table I gives the values of $d_{1\epsilon}$ and

$$P\int d\epsilon'\, d_{2\epsilon'}K_{2\epsilon',1\epsilon}/(\epsilon-\epsilon'-I_{3s}+I_{3p})$$

for several energies $\epsilon$. On the other hand the integral

$$P\int d\epsilon'\, d_{1\epsilon'}K_{1\epsilon',1\epsilon}/(\epsilon-\epsilon'),$$

contributes very little to (9) because $d_{1\epsilon'}$ is small as compared to $d_{2\epsilon'}$ over the energy range considered. Therefore, the energy dependence of the cross section calculated from $D^{(1)}(E)$ can be understood from the magnitude

$$d_{1\epsilon}+P\int d\epsilon'\, d_{2\epsilon'}K_{2\epsilon',1\epsilon}/(\epsilon-\epsilon'-I_{3s}+I_{3p}).$$

At the lower energies, the integral is dominant, but the cross section $[\sim|D^{(1)}(E)|^2]$ decreases very fast because the integral drops very fast with increasing energy $\epsilon$. The minimum in Fig. 1 at the energy ~0.7 a.u. occurs when the two terms are approximately equal but with opposite sign. The further rise of the cross section occurs where $d_{1\epsilon}$ becomes dominant. Eventually the cross section calculated from $D^{(1)}(E)$ and $d_{1\epsilon}$ should nearly coincide.

The analysis of the numerical results in the last paragraph shows how the effect of interchannel interaction manifests itself in the calculation of the photoionization cross section. It also illustrates how the effect of interchannel interaction decreases as the energy increases above the threshold. This calculation shows that interchannel interaction may sometimes substantially upset the picture predicted by an independent-particle approximation.

TABLE I. Contribution of $d_{1\epsilon}$ and $P\int d_{2\epsilon'}K_{2\epsilon',1\epsilon}/(\epsilon-\epsilon'-I_{3s}+I_{3p})\,d\epsilon'$ to the dipole transition amplitude $D^{(1)}$.

| $\epsilon$[a] | $d_{1\epsilon}$ | $P\int \frac{d_{2\epsilon'}K_{2\epsilon',1\epsilon}}{\epsilon-\epsilon'-I_{3s}+I_{3p}}\,d\epsilon'$ |
|---|---|---|
| 0.005 | 0.17929 | −2.3801 |
| 0.105 | 0.22780 | −1.7974 |
| 0.205 | 0.25548 | −1.2981 |
| 0.305 | 0.27417 | −0.91698 |
| 0.405 | 0.28372 | −0.67012 |
| 0.505 | 0.28875 | −0.50112 |
| 0.705 | 0.28832 | −0.29596 |
| 1.005 | 0.26852 | −0.12133 |
| 2.005 | 0.20884 | −0.01312 |

[a] $\epsilon$ is given in a.u. to indicate the energy of the photoelectron in the final states $3s3p^6\epsilon p\,{}^1P^0$ of channel 1.

## IV. IMPROVED RPAE-TYPE CALCULATION

The numerical results of Sec. III give only the qualitative behavior of the cross section for the $3s \to \epsilon p$ transition of Ar, because an analogous calculation for the single-channel $3p \to \epsilon d$ transition in Ar [9] fails to reproduce the experimental result with any accuracy. The main reason for its failure has now been traced to lack of improvement of the initial-state wave function, in view of the success of calculations[14] using random-

TABLE II. Values of $K_{2\epsilon',1\epsilon}$ for Ar. Matrix elements diagonal in $E$ are underlined.

| $2\epsilon'$[b] \ $1\epsilon$[a] | 0.005$p$ | 0.205$p$ | 0.405$p$ | 1.105$p$ | 2.005$p$ |
|---|---|---|---|---|---|
| 3$d$ | 0.037 72 | 0.025 75 | 0.017 21 | 0.005 20 | 0.000 86 |
| 0.0$d$ | 0.351 81 | 0.210 46 | 0.141 66 | 0.044 90 | 0.009 62 |
| 0.5$d$ | <u>0.183 35</u> | 0.116 42 | 0.070 08 | 0.065 20 | 0.032 06 |
| 1.0$d$ | 0.113 89 | 0.069 54 | 0.024 01 | 0.002 10 | 0.020 25 |
| 2.5$d$ | 0.020 99 | 0.021 05 | 0.014 11 | −0.010 61 | <u>−0.041 00</u> |
| 4.0$d$ | −0.014 54 | −0.004 75 | 0.000 52 | 0.002 87 | −0.006 20 |

[a] $1\epsilon$ means values of $\epsilon p$ with $\epsilon$ in a.u. for continuum states $3s3p^6\epsilon p\,{}^1P^0$ of channel 1.

[b] $2\epsilon'$ means $nd$ for discrete states or values of $\epsilon' d$ with $\epsilon'$ in a.u. for continuum states $3s^23p^5\epsilon' d\,{}^1P^0$ of channel 2.

phase approximation with exchange (RPAE) that include such an improvement. Since the calculation of Sec. III depends on the value $d_{3p\to\epsilon d}$ over the whole energy range, we cannot expect its numerical results to predict experimental results correctly. In this section we want to improve the ground-state wave function also, so as to obtain a more-accurate prediction. The qualitative behavior of Fig. 1, i.e., the dip and rapid energy dependence of the cross section near the threshold, should not disappear, but the position of the minimum and the numerical value of the cross section will probably be changed.

Instead of improving the ground-state wave function separately, we improve both initial and final-state wave function simultaneously, using a simplified version of the RPAE method (SRPAE), which is introduced in a companion paper.[15] Briefly speaking, this method permits one to calculate the dipole transition amplitude in a way similar to the reaction-matrix method of Sec. III, yet with a simultaneous improvement of the ground-state wave function. The substantial improvement of the cross section for the $3p\to\epsilon d$ transition calculated by this method[15] permits us to expect the results of this section to be better than those of Sec. III.

According to this simplified RPAE method, the ground-state correlation effect is included by solving the system

$$\bar{K}_{i\epsilon',1\epsilon}=V_{i\epsilon',1\epsilon}+\int d\epsilon''\,V_{i\epsilon',1\epsilon''}\left(\frac{P}{\epsilon-\epsilon''}-\frac{1}{\epsilon+\epsilon''+2I_{3s}}\right)\bar{K}_{1\epsilon'',1\epsilon}$$
$$+\int d\epsilon''\,V_{i\epsilon',2\epsilon''}\left(\frac{P}{\epsilon-\epsilon''-I_{3s}+I_{3p}}-\frac{1}{\epsilon+\epsilon''+I_{3s}+I_{3p}}\right)\bar{K}_{2\epsilon'',1\epsilon}\,, \tag{13}$$

with $i=1,2$, instead of solving Eq. (10). A similar system for $K_{i\epsilon',2\epsilon}$ $(i=1,2)$ is obtained from Eq. (11).

The dipole transition amplitude is then given by

$$\bar{D}^{(1)}(E)=\frac{1-i\pi\bar{K}_{22}}{\bar{\Delta}(E)}\left[d_{1\epsilon}+\int d\epsilon'\,d_{1\epsilon'}\left(\frac{P}{\epsilon-\epsilon'}-\frac{1}{\epsilon+\epsilon'+2I_{3s}}\right)\bar{K}_{1\epsilon',1\epsilon}\right.$$
$$\left.+\int d\epsilon'\,d_{2\epsilon'}\left(\frac{P}{\epsilon-\epsilon'-I_{3s}+I_{3p}}-\frac{1}{\epsilon+\epsilon'+I_{3s}+I_{3p}}\right)\bar{K}_{2\epsilon',1\epsilon}\right]$$
$$+\frac{i\pi\bar{K}_{21}}{\bar{\Delta}(E)}\left[d_{2\epsilon}+\int d\epsilon'\,d_{1\epsilon'}\left(\frac{P}{\epsilon-\epsilon'-I_{3p}+I_{3s}}-\frac{1}{\epsilon+\epsilon'+I_{3p}+I_{3s}}\right)\bar{K}_{1\epsilon',2\epsilon}\right.$$
$$\left.+\int d\epsilon'\,d_{2\epsilon'}\left(\frac{P}{\epsilon-\epsilon'}-\frac{1}{\epsilon+\epsilon'+2I_{3p}}\right)\bar{K}_{2\epsilon',2\epsilon}\right], \tag{14}$$

where $\bar{\Delta}(E)$ is defined as in Eq. (7), with $K_{ij}$ replaced by $\bar{K}_{ij}$. With this choice of $\bar{\Delta}(E)$, we have neglected a contribution to normalization from ground-state correlations. However, this contribution is very small ($\leq 5\%$) as compared to $\bar{\Delta}(E)$.

The result of the cross section calculated by this method for the $3s\to\epsilon p$ transition in Ar is shown in Fig. 1 also. We see that including the improvement of the ground-state wave function reduces the magnitude of the cross section near threshold and moves the minimum of the dip to lower energy. However, as expected, the qualitative behavior of the cross sections calculated by the independent-particle approximation and by the method of Sec. III results from the interchannel interaction between the *final-state* channels; improvement of the *ground-state* wave function does not change this qualitative behavior, even though numerical values do change.

The results of our SRPAE calculation are plotted in Fig. 1, together with those of Sec. III, with those of Amusia *et al.*, and with the experimental data obtained recently by Lynch *et al.*[16] Curve (1) of Amusia *et al.*, from Ref. 5, shows a point of vanishing cross section at a distinctly lower energy than the other results. It has been pointed out later by Amusia[17] that Ref. 5 used an unrealistically higher value of the ionization potential $I_{3s}$ obtained from the Hartree-Fock calculations. Replacement of that value with the experimental one yields the curve (2).

The over-all agreement of the various data is reasonably satisfactory. The remaining discrepancy between the SRPAE results and Amusia's curve (2) derives presumably from differences in the approximation methods. In particular, the SRPAE is based on setting the residual interaction matrix elements $\langle n_1 l_1, n_3 l_3 \| U_1 \| n_2 l_2, n_4 l_4\rangle \sim$

$\langle n_2 l_2, n_3 l_3 \| U_1 \| n_1 l_1, n_4 l_4 \rangle$ in Eq. (6) of Ref. 15. This approximation is quite good for *intra*channel interaction matrix elements, but not as good for *inter*channel interaction matrix elements.

## V. CONCLUSIONS

As was already said in Sec. I, this paper is primarily aimed at studying the effect of interactions between channels upon the partial photoionization cross section of each channel. We have shown that these interchannel interactions have an important influence upon the photoionization cross section, especially for a weak channel near its ionization threshold. We have outlined in Sec. II a general method for studying this effect. The numerical example of the Ar $3s \rightarrow \epsilon p$ transition in Secs. III and IV shows an interaction effect so strong that the oscillator strength of the $3s \rightarrow \epsilon p$ transition is dominated near threshold not by the direct transition process but by coupling with the $3p \rightarrow \epsilon d$ transition. However, we do expect that interchannel effects will show up even if the interaction is not so strong. We also expect that this effect is most prominent near thresholds, because this is the spectral range where singular behavior occurs, as seen in the calculations in Secs. III and IV. In general, interchannel interaction should produce irregularities of the cross section near a threshold, i.e., an energy-dependence trend different from the smoother one prevailing at higher energies.

Measurements of photoionization cross sections for separate channels have been rare up to the present time, especially for channels with smaller cross sections. This kind of experiment should provide a test of the general phenomena indicated above and of different theoretical calculations. Even though there are as yet few experiments that allow us to see the presence of irregularity in the cross section near the threshold as a result of interchannel interaction, there do exist some *ab initio* calculations which permit us to point out these phenomena.

For other rare-gas atoms, the calculations of Amusia *et al.*[5] also show that the cross section of $5s \rightarrow \epsilon p$ transition of Xe has an energy dependence similar to that of Ar in the $3s \rightarrow \epsilon p$ transition, i.e., the cross section near threshold has a rapid energy dependence and a dip, whereas the independent-particle model predicts monotonic rising in that energy range. This example is quite analogous to that of Ar. For Ne $2s \rightarrow \epsilon p$ transition, the result calculated does not have features similar to those of Ar and Xe. However, Fig. 4 of Ref. 5 does show an effect of interchannel interaction; the RPAE calculations, which include interchannel interaction with the $2p \rightarrow \epsilon d$ transition, show an energy dependence near threshold not as sharp as that predicted by the independent particle model. We may understand why the threshold effect is weaker in Ne than in Ar by considering that $d_{2\epsilon}$ is quite smooth in Ne through the $2s$ threshold, in contrast to the case of Ar; presumably the matrices $V_{2\epsilon',1\epsilon}$ and $K_{2\epsilon',1\epsilon}$ are also smoother, yielding a much smaller value of the spectral-repulsion integral

$$P \int d\epsilon' d_{2\epsilon'} K_{2\epsilon',1\epsilon} / (\epsilon - \epsilon' - I_{2s} + I_{2p}).$$

Another example is found in the calculation by Jacobs and Burke[18] of the photoionization cross-section ratio $\sigma(\mathrm{He}^+, n=2)/\sigma(\mathrm{He}^+, n=1)$ in the energy range from the $\mathrm{He}^+$ ($n=2$) threshold (65.4 eV) up to about 200 eV. They find this ratio to have a hump with a maximum at about 75 eV, after which it decreases rather smoothly on the higher-energy side [see Fig. 2(a)]. Because of the availability of accurate ground-state wave functions and of the

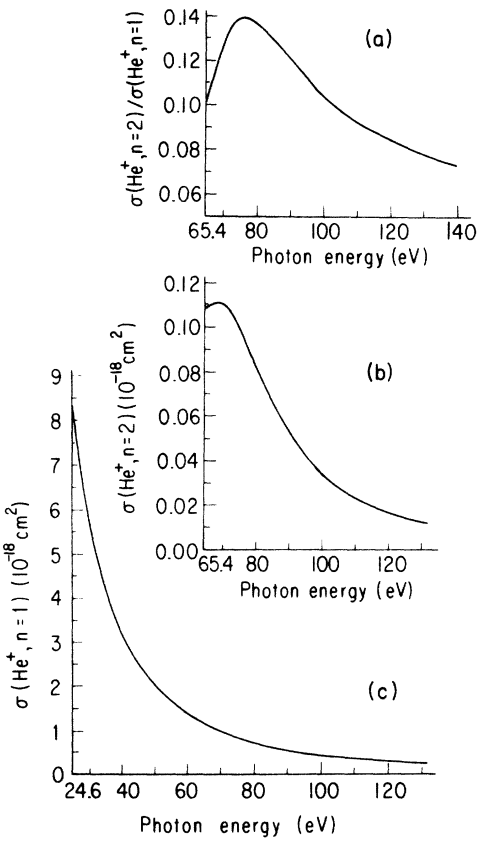


FIG. 2. (a) Photoionization cross-section ratio $\sigma(\mathrm{He}^+, n=2)/\sigma(\mathrm{He}^+, n=1)$ calculated by Jacobs and Burke (Ref. 18); (b) photoionization cross section $\sigma(\mathrm{He}^+, n=2)$; (c) photoionization cross section $\sigma(\mathrm{He}^+, n=1)$, experimental, Ref. 21.

usual accuracy of the close-coupling calculations for the final-state wave function of He, we regard this calculation as reliable. In fact, this calculation has been experimentally confirmed by Krause and Wuilleumier[19] at several energy points between 100 and 200 eV. The existence of the hump near the threshold is not experimentally observed, except for some indications near the $n=2$ threshold.[20] We want to point out that this hump is not surprising in view of the effect of interchannel interaction. We plot in Fig. 2(b) the cross section $\sigma(He^+, n=2)$, taking the ratio of $\sigma(He^+, n=2)/\sigma(He^+, n=1)$ calculated by Jacobs and Burke[18] and $\sigma(He^+, n=1)$ from experimental data[21] [Fig. 2(c)]. We see that the cross section $\sigma(He^+, n=2)$ drops monotonically on the higher-energy side, but also shows a depression near the threshold. The existence of this depression in $\sigma(He^+, n=2)$ and the monotonic decrease of $\sigma(He^+, n=1)$ at this energy region accounts for the hump in the ratio $\sigma(He^+, n=2)/\sigma(He^+, n=1)$. The depression of $\sigma(He^+, n=2)$ near threshold is presumably another example of the effect of interchannel interaction. Therefore, this effect is important not only for channels that have different subshell structures, as in Ne, Ar, Ke, but also for channels that are distinguished by different excitation states of the ion, as in He.

## ACKNOWLEDGMENTS

I would like to express my gratitude to Professor U. Fano for suggesting this problem to me, for his guidance and for many valuable discussions. I am also indebted to Professor A. F. Starace for providing me his residual interaction matrix elements for the $3p \rightarrow \epsilon d$ transition of Ar, and for his helpful communications in the early stages of this work. I also like to thank Dr. M. Ya. Amusia for his comments on the original manuscript.

---

*Work supported by the U. S. Atomic Energy Commission, under Contract No. C00-1674-75, and in part by the National Science Foundation under Grant No. NSF-GH-33636-MRL.

[1]E. Wigner, Z. Phys. 83, 253 (1933); L. D. Landau and E. M. Lifshitz, *Quantum Mechanics* (Pergamon, New York, 1965), p. 565ff.

[2]U. Fano, Phys. Rev. 124, 1866 (1961).

[3]U. Fano and J. W. Cooper, Phys. Rev. 137, A1364 (1965).

[4]U. Fano and J. W. Cooper, Rev. Mod. Phys. 40, 441 (1968).

[5]M. Ya. Amusia, V. K. Ivanov, N. A. Cherepkov, and L. V. Chernysheva, Phys. Lett. A 40, 361 (1972).

[6]J. W. Cooper and S. T. Manson, Phys. Rev. 177, 157 (1969).

[7]F. Herman and S. Skillman, *Atomic Structure Calculations* (Prentice-Hall, Englewood Cliffs, N. J., 1963).

[8]D. J. Kennedy and S. T. Manson, Phys. Rev. A 5, 227 (1972).

[9]A. F. Starace, Phys. Rev. A 2, 118 (1970).

[10]Reference 4, Sec. 6. See also U. Fano and F. Prats, Proc. Natl. Acad. Sci. (India) A 33, 553 (1963).

[11]The linewidths $\Gamma$ of autoionizing states are related to the magnitudes of the interchannel interaction matrix elements. If the two channels are prediagonalized, the linewidth is related to the residual interaction matrix element by $\Gamma_n = 2\pi V^2_{1n,2E}$ for the autoionizing state $|n\rangle$ of channel 1. (See Ref. 2.) If the two channels are not prediagonalized, the linewidth $\Gamma$ is related to the reaction matrix elements by $\Gamma_n = 2\pi K^2_{1n,2E}/(1+\pi^2 K^2_{2E,2E})$. [See F. Prats and U. Fano, in *Atomic Collision Processes*, edited by M. R. C. McDowell (North-Holland, Amsterdam, 1964), p. 600.] From the matrix elements $K_{12}$ and $K_{22}$ calculated in Sec. III at the $3s$ threshold, we obtain $\Gamma_{4p} = 0.042$ eV for the autoionizing state $3s3p^64p\ ^1P$ of Ar. This is to be compared with the experimental value of $\Gamma = 0.08$ eV obtained by R. P. Madden, D. L. Ederer, and K. Codling [Phys. Rev. 177, 136 (1969)]. On the other hand, one can use the experimental linewidth $\Gamma$ to estimate the magnitude of $K_{1E,2E}$ if $K_{2E,2E}$ is obtained by single-channel calculations.

[12]P. L. Altick and E. N. Moore, Phys. Rev. 147, 59 (1966).

[13]U. Fano, F. Prats, and Z. Goldschmidt, Phys. Rev. 129, 2643 (1963), Eq. (29). One can also evaluate the angular factors by graphical method; see J. S. Briggs, Rev. Mod. Phys. 43, 189 (1971).

[14]M. Ya. Amusia, N. A. Cherepkov, and L. V. Chernysheva, Zh. Eksp. Teor. Fiz. 60, 160 (1971) [Sov. Phys.—JETP 33, 90 (1971)].

[15]C. D. Lin, following paper, Phys. Rev. A 9, 181 (1974).

[16]M. J. Lynch, A. B. Gardner, K. Codling, and G. V. Marr, Phys. Lett. A 43, 237 (1973).

[17]M. Ya. Amusia (private communication); in Progress Report at VIII ICPEAC, Belgrade, 1973 (to be published).

[18]V. L. Jacobs and P. G. Burke, J. Phys. B 5, L67 (1972).

[19]M. O. Krause and F. Wuilleumier, J. Phys. B 5, L143 (1972).

[20]See the points of Fano and Cooper and of Samson on Fig. 1 of Ref. 17.

[21]J. F. Lowry, D. H. Tomboulian, and D. L. Ederer, Phys. Rev. 137, A1054 (1965).